

---

# Evaluating Uncertainty Quantification approaches for Neural PDEs in scientific application

---

Anonymous Author(s)

Affiliation

Address

email

## Abstract

1 The accessibility of geographically dispersed data, enabled by affordable sensors,  
2 field and numerical experiments, has led to an abundance of data that can be used  
3 to develop data-driven solutions for scientific problems. Neural Partial Differential  
4 Equations (PDEs), which employ deep learning (DL) techniques alongside domain  
5 expertise in PDEs for parameterization, have proven to be effective in capturing  
6 valuable correlations within spatiotemporal datasets. However, data noise and  
7 sparsity of measurements coupled with model overparameterization introduce  
8 aleatoric and epistemic uncertainties. Therefore, quantifying uncertainties propa-  
9 gated from model inputs to outputs remains a challenge and an essential goal for  
10 establishing the trustworthiness of these method’s predictions. This work evaluates  
11 various Uncertainty Quantification (UQ) approaches, which are crucial for both  
12 Forward and Inverse Problems in scientific applications. Specifically, we investi-  
13 gate the effectiveness of Bayesian methods, such as Hamiltonian Monte Carlo  
14 (HMC) and Monte-Carlo Dropout (MCD), and a more conventional approach,  
15 Deep Ensembles (DE). To illustrate their performance, we take two canonical  
16 PDEs: Burger’s equation and the Navier-Stokes equation. Our results indicate that  
17 these approaches accurately reconstruct flow systems and predict the associated  
18 parameters. However, it is noteworthy that results derived from Bayesian meth-  
19 ods, in our observation, tend to display a higher degree of certainty in predictions  
20 than warranted, as compared to those obtained using the Deep Ensembles (DE)  
21 method. This elevated certainty in predictions implies that Bayesian techniques  
22 might underestimate the actual uncertainty present in the data, thereby appearing  
23 more confident in their predictions than the DE approach.

## 24 1 Introduction

25 The abundant geographically dispersed data facilitated by affordable sensors, numerical and field  
26 experiments, and satellite imagery provided a unique opportunity to tackle ongoing challenges in  
27 climate change, weather prediction, and resilient urban development. However, due to their relatively  
28 low sampling density, the spatiotemporal measurements are limited in providing a comprehensive  
29 view of complex flow systems.

30 While conventional deep learning-based approaches provide promising solutions, they often struggle  
31 to satisfy physical constraints effectively. Physics-Informed Neural Networks (PINNs), as introduced  
32 by Raissi et al. [2019], incorporate physical constraints within the neural network optimization  
33 process, leading to improved physical realizability of the solution. However, due to noisy and limited  
34 data, the accuracy of these models can degrade significantly. [e.g., He and Jiang, 2023]

35 Uncertainty quantification (UQ) in scientific machine learning provides promising avenues to tackle  
36 challenging problem arising due to various factors, such as the stochastic nature of scientific processes,

37 model overparameterization, and data noise. This study aims to compare various UQ techniques,  
 38 including Hamiltonian Monte Carlo (HMC), Monte Carlo Dropouts (MCD), and Deep Ensembles  
 39 (DE) and the robustness of DL techniques. We apply these methods to forward and inverse problems  
 40 in two canonical PDEs - Burger’s and the Navier-Stokes equations, illustrating their performance in  
 41 reconstructing flow systems and predicting unknown parameters from sparse and noisy measurements.

## 42 2 Forward Problems

43 Consider a parameterized and non-linear PDE that characterizes the behavior of a physical system,  
 44 defined as

$$\mathcal{L}_{\mathbf{x}}[\mathbf{u}; \lambda] = \mathbf{f}(\mathbf{x}, t), \mathbf{x} \in \Omega, t \in [0, T], \quad (1)$$

45 where  $\mathbf{u}(\mathbf{x}, t)$  denotes the latent state (aka solution field), the  $\mathcal{L}_{\mathbf{x}}[\cdot; \lambda]$  is a general differential operator  
 46 parameterized by  $\lambda$ ,  $\mathbf{f}(\mathbf{x}, t)$  is the forcing term which refers to any external influences on the system,  
 47 while  $\Omega \subset \mathbb{R}^D$  is the bounded domain in a d-dimensional physical space.

48 Given this framework and noisy measurements of  $\mathbf{u}(\mathbf{x}, t)$ ,  $\mathbf{f}(\mathbf{x}, t)$ , the goal is to infer the latent state  
 49  $\mathbf{u}(\mathbf{x}, t)$  of the dynamical system. In forward problems, PINNs as well as their Bayesian variants  
 50 B-PINNs are typically used as surrogates  $\tilde{\mathbf{u}}(\mathbf{x}, t; \theta)$ , to infer either point estimates or posterior  
 51 distributions of this latent state. In the Bayesian framework, the parameters  $\theta$  of the surrogates have a  
 52 prior distribution  $P(\theta)$  and its formulation is defined as:

$$\tilde{\mathbf{f}}(\mathbf{x}, t; \theta) := \mathcal{L}_{\mathbf{x}}[\tilde{\mathbf{u}}(\mathbf{x}, t; \theta); \lambda] \quad (2)$$

53  $P(\mathcal{D}|\theta)$  represents the likelihood while the Bayes’ Theorem estimates the final posterior distribution.

$$p(\theta|\mathcal{D}) = \frac{P(\mathcal{D}|\theta)P(\theta)}{P(\mathcal{D})} \cong P(\mathcal{D}|\theta)P(\theta) \quad (3)$$

54 To approximate the posterior distribution, we employ both Bayesian methods like HMC and MCD  
 55 as well as deterministic DE approach. HMC is an efficient Markov Chain Monte Carlo (MCMC)  
 56 sampling method that uses concepts from Hamiltonian Dynamics and utilizes momentum variables to  
 57 guide the proposals in the Markov chain, which can lead to faster convergence and better exploration  
 58 of the target distribution. Given the continuous nature of Hamiltonian dynamics, leapfrog integration  
 59 is used as a numerical technique to discretize and update the momentum and position variables in a  
 60 staggered manner over discrete time steps. In our Bayesian methodology, we posit an independent  
 61 Gaussian distribution as the prior  $P(\theta)$ . For HMC, parameters for Burger’s (Navier-Stokes) equation  
 62 include a leapfrog step of 50 (50), an initial time step of 0.1 (0.01), 1000 (5000) burn-in steps, and a  
 63 sampling size of 100 (100). With DE, we assemble an ensemble of PINNs equivalent in number to  
 64 the HMC samples, set at 100 (200). For MCD, we induce variance by sporadically dropping neurons  
 65 at a 1% (1%) dropout rate during each training iteration. To gauge prediction uncertainty, we execute  
 66 100 (200) inferences with HMC. For DE, we acquire 100 (200) predictions from each ensemble  
 67 member, and for MCD, we undertake forward network propagation 100 (200) times, maintaining the  
 68 established dropout rate.

### 69 2.1 1-D Burger’s Equation

70 Burger’s equation is a PDE that represents a combination of diffusion and convection processes. It  
 71 has wide applications in various scientific domains, including traffic flow modeling, acoustics, and  
 72 sound propagation, and material transport in porous media. here, we consider a one-dimensional  
 73 Burger’s equation with Dirichlet boundary condition and sinusoidal initial conditions as follows:

$$\begin{aligned} \frac{\partial u}{\partial t} + u \cdot \nabla u - \frac{0.01}{\pi} \nabla^2 u &= 0, \quad x \in [-1, 1], t \in [0, 1], \\ u(0, x) &= -\sin(\pi x), \\ u(t, -1) = u(t, 1) &= 0, \end{aligned} \quad (4)$$

75 where  $x$  and  $t$  is the spatial location and time,  $u(x, t)$  is the velocity of the fluid, and  $\nabla$  and  $\nabla^2$   
 76 represents gradient and Laplacian operators.

77 Chebfun package has been employed to exact solution and for more details, please refer Rico-Martinez  
 78 et al. [1994] and Raissi et al. [2019]. Here, we assume an unknown exact solution and instead use

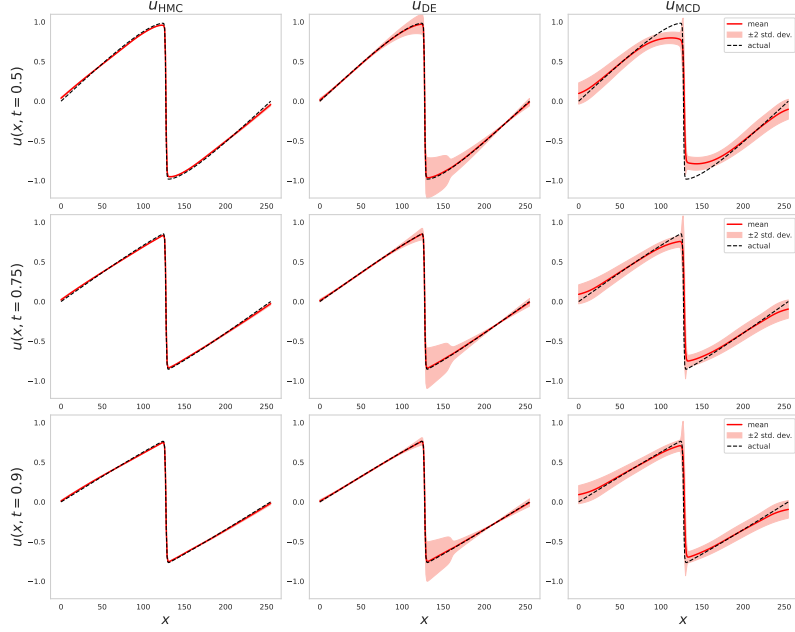


Figure 1: One-dimensional Burgers equation - forward problem: comparison of the predicted and exact solutions corresponding to the three temporal snapshots denoted by  $t \in \{0.50s, 0.75s, 0.90s\}$  from different methods.

79 noisy sensors to collect 2000 spatiotemporal readings for  $u$  and  $f$ . The sensor measurements have  
80 Gaussian noise with scales  $\epsilon_f$  and  $\epsilon_u$  as  $\mathcal{N}(0, 0.1^2)$ . A multilayer perceptron (MLP) neural  
81 network consisting of eight hidden layers, each comprising 20 neurons with tanh non-linearity is  
82 employed to approximate the solution.

83 The predictive means ( $\mu$ ) and the corresponding two standard deviations ( $\pm 2\sigma$ ) using three different  
84 methods, HMC, MCD, and DE at three distinct time snapshots, particularly  $t \in \{0.50s, 0.75s, 0.90s\}$   
85 is illustrated in figure 1. From visual inspection, it is evident that both the HMC and DE approaches  
86 provide reasonably accurate posterior estimations of the variable  $u$  at all three time-snapshots.  
87 Moreover, the error between these predictive means and the actual solution remains predominantly  
88 within  $\pm 2\sigma$ . In contrast, the MCD approach exhibits discrepancies from the actual solution across all  
89 temporal snapshots, although these discrepancies tend to diminish as time progresses. It is noteworthy  
90 that, for  $t = 0.50s$ , a significant portion of the error falls outside the two standard deviation confidence  
91 intervals. However, as time advances, the performance of the MCD approach noticeably improves. It  
92 is also important to highlight that all three approaches effectively capture the formation of shocks, a  
93 challenging task even for classical numerical methods.

## 94 2.2 2-D Navier Stokes Equation

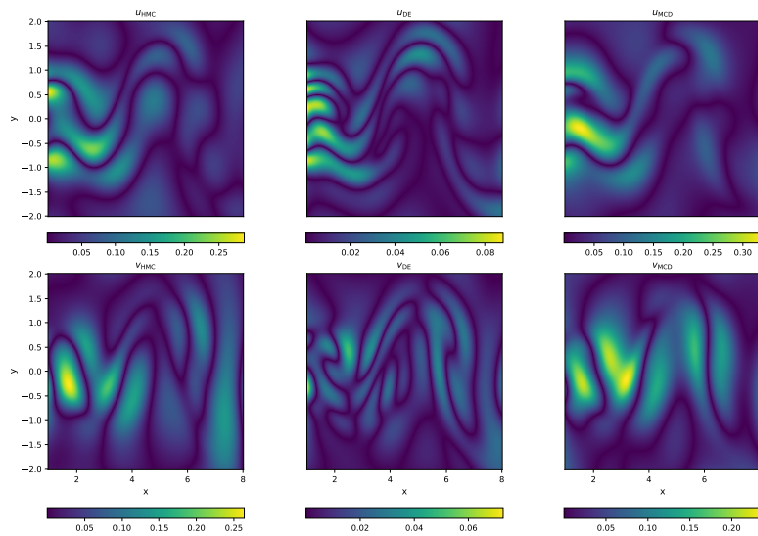
95 In our next example, we explore the practical scenario of incompressible fluid flow described by  
96 the Navier-Stokes equations. These equations are fundamental in science and engineering, with  
97 applications in various fields like climate prediction, aerodynamics, and blood circulation. An  
98 incompressible flow past a cylinder case is considered, and the associated governing equation are  
99 defined as follows:

$$\frac{\partial \mathbf{u}}{\partial t} + \lambda_1 \mathbf{u} \cdot \nabla \mathbf{u} + \nabla \mathbf{u} - \lambda_2 \nabla^2 \mathbf{u} = 0, \quad (5)$$

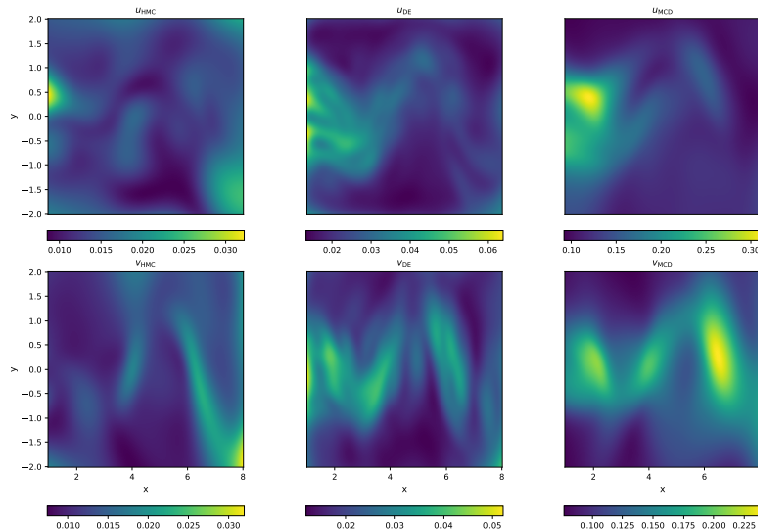
100

$$\nabla \cdot \mathbf{u} = 0,$$

101 where  $\mathbf{u} = \{u, v\}$  and  $p$  are the 2-D velocity and pressure fields,  $t$  is time, and  $\lambda = \{\lambda_1, \lambda_2\}$  are the  
102 parameters and for the forward problems  $\lambda_1$  is set to 1 and  $\lambda_2$  to  $10^{-2}$ . Given the multidimensional  
103 nature of this problem, it offers a challenging testbed for the Bayesian approach to quantify uncertain-  
104 ties in both the  $\mathbf{u}$  and  $p$  fields. It is important to emphasize that  $p$  measurements are not included in



(a) Predictive errors for velocity component in  $x$ -direction  $u$  (top) and  $y$ -direction  $v$  (bottom) from different methods at a representative time instant.



(b) Two standard deviations ( $\sigma$ ) for velocity component in  $x$ -direction  $u$  (top) and  $y$ -direction  $v$  (bottom) from different methods at a representative time instant.

Figure 2: Navier-Stokes equation - forward problem.

105 the model training; instead, the neural network predicts them based on the governing equation. To  
 106 generate the exact solutions, we leverage the data provided for the work by Raissi et al. [2019], and  
 107 readers are advised to refer to the same for more details. Similar to section 2.1, noisy sensors capture  
 108 5000 spatiotemporal readings for both  $u$  and  $f$  with Gaussian noise  $\mathcal{N}(0, 0.1^2)$ . A 10-layer MLP  
 109 network with 20 neurons per layer and a tanh non-linearity is used to approximate the latent variables  
 110 ( $u$ ,  $v$ , and  $p$ ).

111  $L_1$  norm-based error  $\epsilon$  between the actual and predictive  $\mu$  values and  $\pm 2\sigma$  are presented in figure 2a.  
 112 Notably, the DE approach exhibits the closest agreement with the actual solutions. In contrast, the  
 113  $\epsilon_{\text{HMC}}$  and  $\epsilon_{\text{MCD}}$  approaches are roughly three times higher than  $\epsilon_{\text{DE}}$  for  $\mathbf{u}$  field. The  $\epsilon$  consistently  
 114 remains within the  $\pm 2\sigma$  for all considered methodologies, as illustrated in figure 2b and underscores  
 115 our confidence in the predictions generated using various approaches, as they remain well within the  
 116 established confidence interval.

### 117 3 Inverse Problems

118 Inverse problems involve determining a system's underlying parameters  $\lambda$  and physical properties  
 119 from observable data. This study offers a systematic approach to quantify uncertainties in estimating



120 unknown parameters for the Navier-Stokes equation (5). Similar to the framework described in  
 121 equations [2-3] **update this**, apart from a surrogate for  $\theta$ , we also assign a prior distribution for  $\lambda$ ,  
 122 which can be independent of the prior for  $\theta$ . The likelihood is then defined as  $P(\mathcal{D}|\theta, \lambda)$ , and we then  
 123 calculate the joint posterior of  $[\theta, \lambda]$ :

$$p(\theta, \lambda|\mathcal{D}) = \frac{P(\mathcal{D}|\theta, \lambda)P(\theta, \lambda)}{P(\mathcal{D})} \cong P(\mathcal{D}|\theta, \lambda)P(\theta, \lambda) = P(\mathcal{D}|\theta, \lambda)P(\theta)P(\lambda) \quad (6)$$

	HMC	DE	MCD
$\lambda_1$ (mean $\pm$ std)	$0.758 \pm 0.0$	$0.957 \pm 0.024$	$0.843 \pm 0.075$
$\lambda_2$ (mean $\pm$ std)	$0.017 \pm 2.13e-06$	$0.014 \pm 0.001$	$0.015 \pm 0.058$

Table 1: Navier Stokes equation - inverse problem : Predictions for  $\lambda_1, \lambda_2$  using HMC, DE, MCD; actual values for  $\lambda_1 = 1.0, \lambda_2 = 0.01$

124

125 The primary objective is to estimate  $\lambda = \{\lambda_1, \lambda_2\}$  and associated uncertainty based on the limited  
 126 measurements of  $f$  and  $\mathbf{u} = [u, v]$  outlined in section 2.2. To do so, we employ the MLP model  
 127 of ten hidden layers with 40 neurons in each layer and tanh non-linearity. The predicted values of  
 128  $\lambda$ 's are displayed in Table 1. The DE method has provided relatively precise estimates, reflecting a  
 129 good degree of certainty in its predictions. This suggests that ensemble techniques effectively capture  
 130 these parameters' underlying distributions. While HMC provides high confidence in its estimates,  
 131 the absence of uncertainty is unrealistic, and this overconfidence could be a sign of the model not  
 132 capturing all sources of uncertainty. MCD provides a broader uncertainty estimation, which might be  
 133 capturing more sources of uncertainties, but it could also be overestimating the uncertainty in the  
 134 parameters. The wider confidence intervals for MCD could either mean that MCD is being more  
 135 cautious or it's not as effective in pinpointing the true parameter values. These findings underscore the  
 136 effectiveness of the DE approach in not only identifying the unknown parameters but also quantifying  
 137 the uncertainty arising from the sparse and noisy sensor measurements.

## 138 4 Summary

139 This study compares and evaluates various UQ approaches, particularly Bayesian and Deep Ensemble  
 140 (DE) techniques. While all approaches, including DE, HMC, MCD, effectively reconstruct flow  
 141 systems and predict unknown parameters for the two examples considered, Bayesian methods  
 142 demonstrate higher certainty in predictions but may underestimate the total uncertainty, thereby  
 143 appearing overly confident. In contrast, while offering more conservative certainty estimates, the DE  
 144 method is computationally taxing. The study underscores the need for balancing predictive certainty,  
 145 computational efficiency, and accuracy when using Bayesian or DE approaches for flow system  
 146 modeling and parameter prediction.

## 147 References

- 148 Maziar Raissi, Paris Perdikaris, and George E Karniadakis. Physics-informed neural networks: A  
 149 deep learning framework for solving forward and inverse problems involving nonlinear partial  
 150 differential equations. *Journal of Computational physics*, 378:686–707, 2019.
- 151 Wenchong He and Zhe Jiang. A survey on uncertainty quantification methods for deep neural  
 152 networks: An uncertainty source perspective. *arXiv preprint arXiv:2302.13425*, 2023.
- 153 R Rico-Martinez, JS Anderson, and IG Kevrekidis. Continuous-time nonlinear signal processing: a  
 154 neural network based approach for gray box identification. In *Proceedings of IEEE Workshop on  
 155 Neural Networks for Signal Processing*, pages 596–605. IEEE, 1994.